



## Fabrication and Performance Analysis of Nafion-based IPMC Actuator

Shahla.Eskandarishahraki<sup>1</sup> - Mahdie.Fatollahi<sup>1</sup> - Arash.Payami<sup>1</sup> - Mohammad.Reza. Daraei<sup>2,\*</sup>

<sup>1</sup> Polymer Engineering Department, Faculty of Materials and Manufacturing Technologies, Malek Ashtar University of Technology, Tehran, Iran

<sup>2</sup> Polymer Engineering Department, AmirKabir University of Technology (Tehran Polytechnic), Tehran, Iran

### ABSTRACT

*Ionic Polymer-Metal Composites (IPMCs) are a type of smart material with layered structures consisting of an electrode/ion-exchange membrane/electrode configuration. Owing to their large bending deformations at very low voltages, lightweight nature, and ease of fabrication, they are considered an ideal option for applications such as artificial actuators, sensors, and energy harvesters. In this study, an IPMC actuator was fabricated by depositing platinum metal electrodes onto an ion-exchange Nafion membrane.*

*Based on the results of scanning electron microscopy, the formation of the metal electrode layer was confirmed, and the thickness of the deposited electrodes was measured to be approximately 11-12  $\mu\text{m}$ . The water absorption capacity and electrode surface resistance of the IPMC actuator, which directly influence its performance, were investigated over time. With repeated expansion and contraction of the actuator during operation, structural defects on the electrode surfaces, such as cracks and fractures, grow deeper, resulting in a gradual decline in the actuator's performance. Functional parameters such as actuator's displacement, operational stability and blocking force were tested under various voltages. At an input voltage of 4 V, the tip displacement of the IPMC with dimensions of  $2 \times 6 \text{ cm}^2$  was measured to be 40 mm, and its operational duration in air was about 20 minutes. Additionally, blocking force, under the mentioned voltage was calculated to be approximately 6.4 gf.*

**Keywords:** Smart materials, Actuator, Ionic polymer-metal composites (IPMC), Ion-exchange polymers

### 1. INTRODUCTION

*Ionic Polymer-Metal Composites (IPMCs) have emerged as a highly promising class of electroactive materials, capturing the interest of researchers and engineers owing to their unique ability to exhibit large bending deformations under low applied voltages. This characteristic makes them particularly suitable for applications in soft robotics, biomedical devices, and artificial muscles, where precise, responsive, and energy-efficient actuation is critical [1,2]. IPMCs typically consist of an ion-exchange membrane, such as Nafion, sandwiched between two metal electrodes. When an electric field is applied, the migration of hydrated cations within the membrane induces mechanical deformation, enabling these materials to function as effective actuators or sensors. This combination of electrical responsiveness and mechanical flexibility has positioned IPMCs as a key enabling technology for next-generation innovations in robotics, healthcare, and energy systems. Over the past two decades, extensive research has been conducted to understand the underlying mechanisms of IPMC actuation, optimize their performance, and explore their potential in various applications [3,4].*

*The ion-exchange membrane is a critical component of IPMCs, with Nafion being the most widely used material due to its exceptional ionic conductivity, mechanical flexibility, and chemical stability. Nafion, a perfluorosulfonic acid polymer, facilitates the movement of hydrated cations, which is essential for the actuation mechanism of IPMCs. However, the performance of IPMCs is influenced by several factors, including the quality of the electrode layer, the properties of the ion-exchange membrane, and the operating conditions. Platinum is commonly employed as the electrode material in IPMCs due to its excellent electrical*

conductivity and chemical stability. Despite these advantages, challenges such as electrode cracking, solvent loss, and performance degradation under cyclic loading have hindered the widespread adoption of IPMCs in practical applications [5,6]. These issues underscore the need for continued research into material optimization and fabrication techniques to enhance the durability and reliability of IPMCs.

Recent advancements in fabrication methods, particularly electroless plating, have shown promise in addressing some of these challenges. Electroless plating enables the uniform deposition of metal electrodes onto the ion-exchange membrane, improving interfacial adhesion and overall performance. Optimizing the electroless plating process can significantly enhance the electrode-membrane interface, resulting in IPMCs with improved actuation performance and durability [7]. Additionally, researchers have focused on understanding the relationship between key functional parameters, such as displacement, generated force, and durability, under varying operating conditions. These studies aim to optimize the electromechanical performance of IPMCs, making them more suitable for real-world applications [8].

The ability of IPMCs to generate precise and controllable movements has been leveraged in various applications. For example, in soft robotics, actuators based on IPMCs have been employed to create robotic grippers designed to handle delicate objects with precision. In the biomedical field, their biocompatibility and low operating voltages make them ideal candidates for drug delivery systems, prosthetics, and even artificial muscles for rehabilitation devices [9]. Furthermore, IPMCs have shown potential in energy harvesting systems, where their ability to convert mechanical energy into electrical energy can be utilized to power low-energy. These diverse applications underscore the versatility and transformative potential of IPMCs [8,9].

In this study, platinum metal electrode layers were deposited on a Nafion 115 membrane using an electroless plating method to fabricate a  $2 \times 6 \text{ cm}^2$  IPMC actuator. The structural properties, including thickness, surface topography, and surface resistance of the electrodes, as well as key functional parameters of the actuator such as tip displacement, functional stability, and blocking force, were investigated using various analytical techniques. The findings of this research not only provide a deeper understanding of the electromechanical behavior of Nafion-based IPMC actuators but also pave the way for optimizing their design and performance in emerging applications such as soft robotics, biomedical devices, and energy harvesting systems. This study represents a significant step toward the development of advanced technologies with enhanced operational capabilities.

## 2. EXPERIMENTAL SECTION

### 2.1 Materials

Nafion 115, the base polymer membrane utilized in the study, was sourced from DuPont. Tetraammine platinum(II) chloride hydrate ( $[\text{Pt}(\text{NH}_3)_4]\text{Cl}_2 \cdot x\text{H}_2\text{O}$ ) was acquired from Sigma-Aldrich. Sodium borohydride ( $\text{NaBH}_4$ ) was used as the primary reducing agent and hydrazine hydrate ( $\text{NH}_2\text{NH}_2 \cdot 1.5\text{H}_2\text{O}$ ) and hydroxylamine hydrochloride ( $\text{NH}_2\text{OH} \cdot \text{HCl}$ ) were used as secondary reducing agents, all of which were obtained from Merck (Germany).

A diluted ammonium hydroxide solution ( $\text{NH}_4\text{OH}$ , 5% solution) and diluted hydrochloric acid solutions ( $\text{HCl}$  aq., 2 N and 0.1 N solutions) was prepared in Polymer Research Laboratory at Amirkabir University of Technology, Iran. Lithium chloride ( $\text{LiCl}$ ) was obtained from Merck (Germany). Other essential materials and equipment for the process included deionized water, 2000# sandpaper, an ultrasonic cleaner, an electronic weighing balance, a beaker, a magnetic stirrer with a hot plate, and standard laboratory glassware.

### 2.2 Manufacturing of ionic polymer metal composite

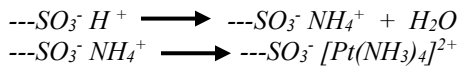
IPMC actuators were prepared from Nafion 115 membrane with dimensions of  $20 \times 60 \times 0.125 \text{ mm}^3$  according to the following steps:

#### 2.2.1. Pretreatment of Nafion membrane:

First, the surface of the membrane was roughened using 2000# sandpaper to increase the contact area and allow more platinum ions to deposit on the Nafion membrane during the reduction steps. The membrane was then placed in deionized water and cleaned using an ultrasonic cleaner for 1 hour at  $45^\circ\text{C}$  to remove particles and impurities generated during the sanding process. Subsequently, the membrane was boiled in a 2 N  $\text{HCl}$  solution for 30 minutes, followed by boiling in deionized water for another 30 minutes to remove the acid.

### 2.2.2. Ion exchange process:

The platinum salt solution was prepared by dissolving 130 mg of the platinum complex  $[Pt(NH_3)_4]Cl_2 \cdot xH_2O$  in 52 ml of distilled water (resulting in a concentration of 2.5 mg of platinum per milliliter). Then, 1 ml of a 5% wt aqueous ammonium hydroxide solution was added to the mixture. The Nafion membrane was immersed in the prepared solution for 24 hours to allow the ion exchange process of  $[Pt(NH_3)_4]^{2+}$  ions.



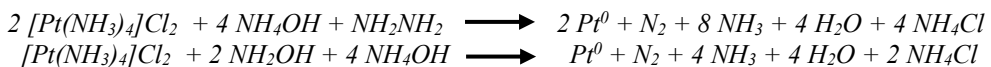
### 2.2.3. Primary reduction:

After removing the membrane from the platinum salt solution, it was rinsed with deionized water. The membrane was then placed in 180 ml of water, which was being stirred, inside another water bath maintained at 40°C. To reduce the platinum cation complexes to their metallic state and form a metallic layer, 5 ml of a 5% wt aqueous sodium borohydride ( $NaBH_4$ ) solution was added to the system every 10 minutes over a period of 4 hours (24 times in total). During these 4 hours, the temperature of the water bath was gradually increased to 60°C. After the 4-hour period, an additional 20 ml of the 5% wt  $NaBH_4$  solution was added, and the system was kept stirring at 60°C for 1.5 hours. At this stage, a black layer formed on the membrane. The Nafion membrane was then rinsed with deionized water and immersed in a 0.1 N HCl solution for several hours. By the end of the first reduction step, a small amount of platinum had been deposited on the membrane.



### 2.2.4. Secondary reduction:

To enhance the performance of the IPMC, an additional layer of platinum was deposited on the membrane during the second reduction step. For this purpose, an aqueous solution of the platinum complex salt was prepared by dissolving 120 mg of the salt in 240 mL of deionized water, and 5 mL of a 5% ammonium hydroxide solution was added to it. The membrane was then immersed in this solution, which was stirred at 40°C. Subsequently, every 30 minutes over a period of 4 hours, 6 mL of a 5% hydroxylamine hydrochloride solution and 3 mL of a 20% hydrazine hydrate solution were added, while the temperature of the system was gradually increased to 60°C. To check the endpoint, a small amount of the solution was gently heated with  $NaBH_4$ . Safety precautions must be strictly followed during this step, as adding  $NaBH_4$  powder to a hot solution can cause gas explosions. If any traces of Pt ions remain in the solution, the solution will turn black. In such a case, the development of the metallic layer continues by adding reducing agents until no Pt ions remain in the solution. The IPMC was rinsed with deionized water and boiled in a 0.1 N HCl solution for 30 minutes to remove ammonium cations. It was then rinsed again with deionized water and immersed in a saturated lithium chloride ( $LiCl$ ) solution to facilitate cation exchange. The  $H^+$  in the composition can be exchanged with any cation by immersing it in a chloride salt solution of the desired cation, such as  $LiCl$ , to convert it into the lithium cation form. Finally, the fabricated IPMC actuator was washed and stored in deionized water.



## 2.3. IPMC Analyses Methods

### 2.3.1. Scanning Electron Microscopy

To confirm the formation of metallic electrode layers on the Nafion membrane and to analyze their surface topography, SEM imaging was performed. Prior to testing, the samples were immersed in liquid nitrogen for several minutes to induce brittleness. Subsequently, the samples were fractured by applying mechanical force. A critical step in the preparation process for this analysis involves coating the test surfaces with a conductive metal, typically gold, to prevent charge accumulation. However, in these samples, since a deposition process has been conducted and a thin layer of platinum metal is already present on the surfaces of the Nafion membrane, this step is unnecessary. The SEM analysis was performed using the Tescan Vega-III instrument.



### 2.3.2. Water uptake capacity

The water absorption parameter of IPMC actuators significantly impacts their functional properties. The change in weight of the wetted membrane after water absorption is used to calculate the water uptake capacity of the fabricated IPMC. A pre-weighed IPMC strip (dried at 25°C) was immersed in distilled water at room temperature (25°C) for different time intervals (2, 4, 6 hours, etc.). After wiping the surface, the weight of the membrane was measured. Based on the measured weights and using the following formula, the water absorption capacity of the membrane was calculated:

$$WUP = ((W_{\text{wet}} - W_{\text{dry}}) / W_{\text{dry}}) \times 100\%$$

Where  $W_{\text{wet}}$  is the weight of the wet membrane after immersion and  $W_{\text{dry}}$  is the weight of the dry membrane before immersion.

### 2.3.3. Surface resistance of electrodes

Using a VICTOR VC96 digital multimeter, the surface resistance of a platinum-coated IPMC with dimensions of  $20 \times 60 \text{ mm}^2$  was determined. The resistance between two points at varying distances from the edge of the IPMC was measured. Additionally, the change in surface resistance of the IPMC were measured over time at a constant distance. Each measurement test was repeated five times, and the average of the results was reported.

### 2.3.4. Tip displacement

For analyzing the bending characteristics, about 1 cm of a IPMC strip with dimension of  $20 \times 60 \text{ mm}^2$  was fixed using copper electrodes (with two wires connected to power supplier), while the other end was left free to bend. The bending displacement of the IPMC tip was measured using graph paper under DC voltage supplied by a power source (a direct current generator from DAZHENG, model PS-305D). The input voltage was varied between 0.5 and 4 V, and the corresponding change curves were plotted.

### 2.3.5. Blocking force

The IPMC actuator was fixed at one end to copper electrodes connected to a direct power supply, while the other end was free to touch the tip of the conical element on a digital scale. The blocking force of the IPMC, under different DC voltages, was calculated by measuring the change in the weight displayed on the scale.

### 2.3.6. lifting capacity

To evaluate the maximum load capacity of the IPMC actuator, small objects with predetermined weights were placed on the actuator connected to a 4 V direct current. The number of weights was then gradually increased until reaching the maximum amount that the IPMC strip could lift.

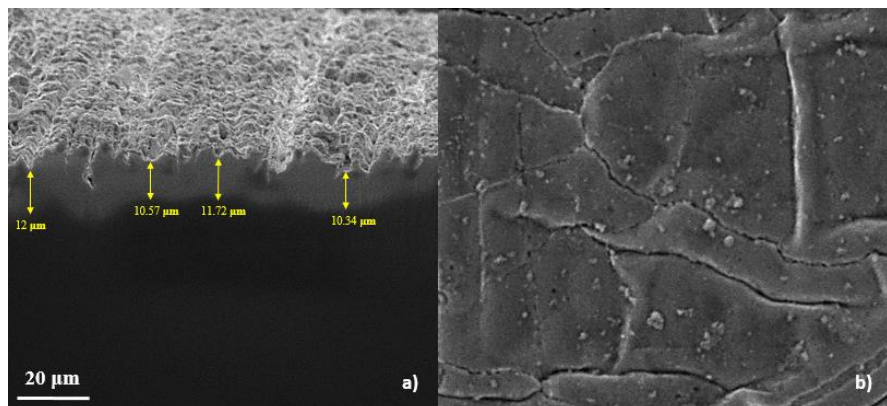
### 2.3.7. Functional stability in air

One of the most critical factors for the application of this class of smart materials across various industries is their functional stability under diverse environmental conditions. To assess this, an IPMC strip of  $2 \times 6 \text{ cm}^2$  was immersed in deionized water for 24 hours to achieve water equilibrium. Subsequently, the IPMC strip was connected to a direct power supply using copper electrodes and current wires. The input voltage was set to 4 V, a level that induced maximum displacement while also causing the highest rates of solvent evaporation and electrolysis. The current was applied until the strip reached its peak displacement, after which the current was cut off, allowing the strip to return to its initial position, effectively relaxing. This cycle was repeated intermittently until the displacement of the IPMC strip diminished to nearly zero. By plotting the displacement versus time curve and documenting the process through video recordings, the functional stability of the prepared strip was evaluated.



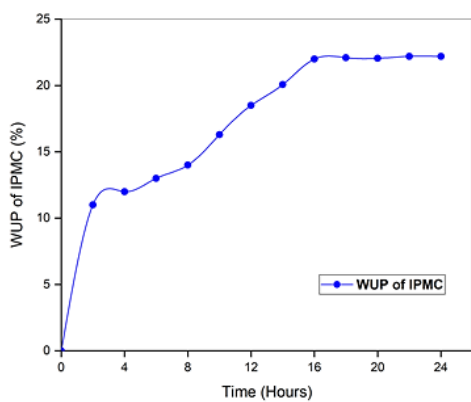
### 3. RESULT AND DISCUSSION

Figure 1 displays the SEM micrographs of the cross-sectional view of the IPMC and the surface topography of its metallic electrode layer. The images clearly indicate that platinum particles were uniformly deposited on the ion-exchange membrane during the reduction processes. From the cross-sectional image of the IPMC (Figure 1a), the thickness of the metallic electrode layer was measured to be approximately 11-12  $\mu\text{m}$ , which is expected to provide suitable electrical conductivity. Furthermore, the surface topography images taken at very small scales (Figure 1b), clearly reveal the presence of cracks and fractures on the platinum electrode surfaces. The formation pattern of these cracks and fractures is influenced by the membrane's pre-treatment process, particularly different surface roughening methods. Over time and during the operation of these actuators, the brittle nature of the metal electrodes causes the cracks and fractures to grow deeper. These structural defects can lead to an increase in surface resistance of electrodes and an accelerated rate of solvent loss, ultimately diminishing the performance of the IPMC [10-13].



**Figure 1.** SEM images of the a) cross section of the Nafion IPMC and b) surface morphology of the Pt electrode

The water uptake (WUP) values of the Nafion-based IPMC at various time intervals are presented in Figure 2. At 25°C, the WUP value of the IPMC was approximately 11% after 2 hours of immersion in water. As shown, the WUP values increased at a relatively constant rate from 2 to 16 hours, eventually reaching a saturation level of approximately 23% [14, 15]. Since the performance of the IPMC actuator is directly influenced by its solvent (water) content, this curve can be used to determine the time required to reach equilibrium state and achieve optimal actuator performance.



**Figure 2.** Variation of water uptake capacity over time

The surface resistance values of the Pt electrodes along the length of the IPMC is shown in Figure 3. At distances of 10, 20, 30, 40, and 50 mm from the tip, the surface resistance values were calculated as 6.5, 7.9,

9.6, 11.2, 14.5, and 15.8  $\Omega$ , respectively. As the distance from the beginning of the strip increases, the surface resistance rises due to an increase in structural defects related to fabrication methods, impurities, and other factors.



**Figure 3.** Surface resistance of the Pt electrode along the length of the IPMC

The surface resistance values of the platinum electrodes indirectly indicate the degree of uniformity of these electrodes. The lower the surface resistance values, the better the uniformity and distribution of the metal particles. Figure 4 shows the variation in surface resistance values over time during the operation of the IPMC (sequential contractions and expansions) at a fixed distance of 10 mm. As observed, the surface resistance of the electrodes increases over time following repeated back-and-forth movements of the actuator. In the initial stages, the rate of increase in surface resistance is steeper due to greater deformation of the IPMC strip. However, as deformation (contraction and expansion) diminishes over time because of solvent loss, the rate of increase in surface resistance also slows down [16-18]. Repeated contractions and expansions of the IPMC induce structural defects, such as cracks and fractures, on the metal electrode surfaces, which reduce the uniformity of the electrode particles. This leads to an increase in the surface resistance of the electrodes and a gradual decrease in their deformation over time.

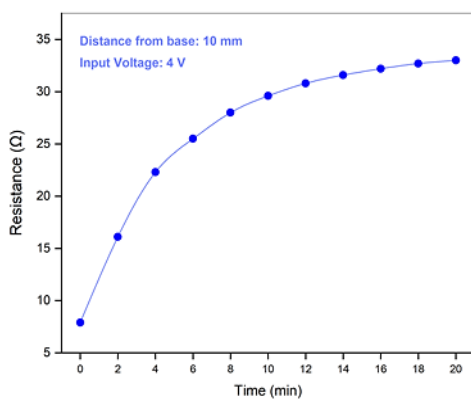


**Figure 4.** Surface resistance of the Pt electrode as a function of time

The displacement of the IPMC tip under applied DC voltages ranging from 1 to 4 V is illustrated in Figure 5. When the input voltage is set to 0.5 V, the IPMC remains stationary, and its displacement is zero. As the voltage increases to 1 V, the tip begins to move, achieving a displacement of 2 mm from its initial position. However, this displacement still does not meet the required specifications. When the voltage is further increased to 2, 3, and 4 V, a significant rise in both displacement and bending angle of the actuator strip is

observed. This occurs despite the accelerated rate of solvent loss caused by evaporation and electrolysis. The enhanced displacement is attributed to the increased migration rate of hydrated cations, resulting in a notable displacement of approximately 40 mm at an input voltage of 4 V. Consequently, optimizing the input voltage to achieve substantial displacement while minimizing solvent loss is one of the most critical functional requirements for this class of smart materials [19-23].

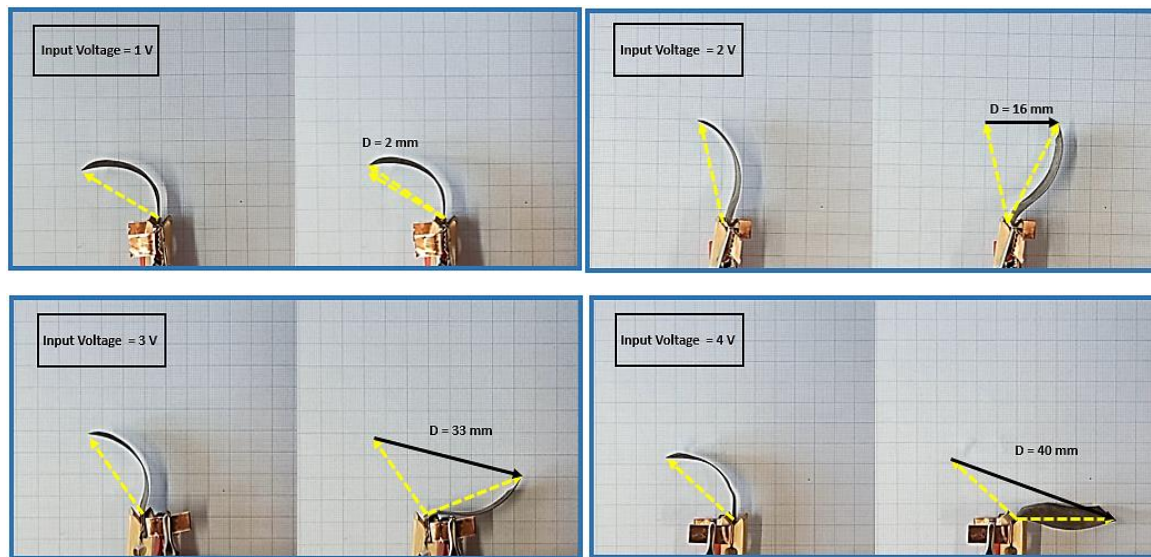


Figure 5. Tip displacement of the IPMC under various DC voltages

The blocking force of the IPMC actuator was measured using the system depicted in Figure 6. As shown, when a direct voltage is applied, the actuator strip, which is fixed onto a holder, moves downward and makes contact with the surface of a conical object. The weight of this object had previously been zeroed on the scale. This contact produces a force that results in a change in the weight displayed on the scale [24,25].

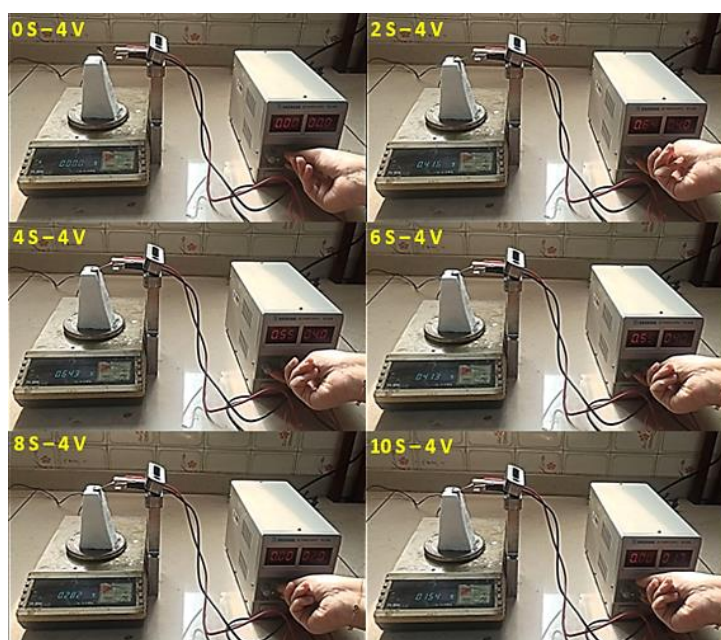


Figure 6. Blocking force measurement of the IPMC under a 4 V DC

The generated force, initially increased over time, reaching its peak value within the first 4 seconds. Following this, from 4 to 10 S, as the current is interrupted and the IPMC strip relaxes, the force gradually decreases, returning to its initial level. The time-dependent variation of the blocking force at an input voltage of 4 V is illustrated in Figure 7 [26].

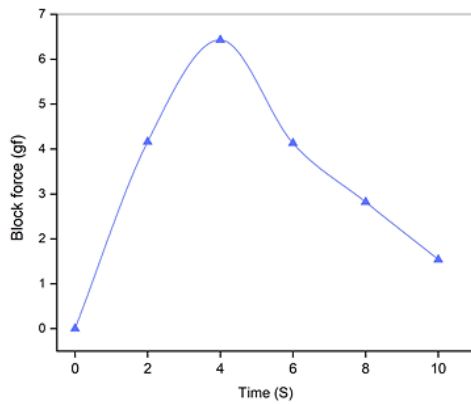


Figure 7. Blocking force as a function of time under a direct applied voltage of 4 V

To investigate the relationship between the blocking force and the input voltage, the blocking force values was plotted as a function of input voltages (Figure 8). As observed, the blocking force increased with higher input voltages. This is attributed to the enhanced speed of hydrated cation transfer within the Nafion membrane, which results from the increased voltage [27].

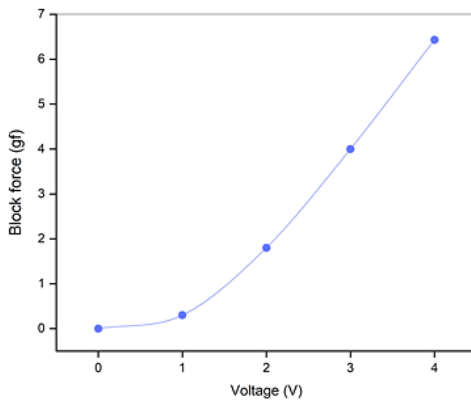


Figure 8. Blocking force as a function of voltage

Figure 9 illustrates the lifting capacity of a  $2 \times 6 \text{ cm}^2$  IPMC strip when operated at 4 V. The actuator was able to lift 5 pieces with a total weight of 0.54 g in just 4 seconds. Additionally, the lifting capacity was tested across input voltages ranging from 0 to 4 V, with results showing capacities of 0, 0.33, and 0.46 g at 1, 2, and 3 V, respectively. Given that the dry IPMC actuator itself weighs approximately 0.44 g, it is evident that this class of smart actuator materials exhibits a high power-to-weight ratio, establishing it as a critical parameter for a wide range of applications [28,29].

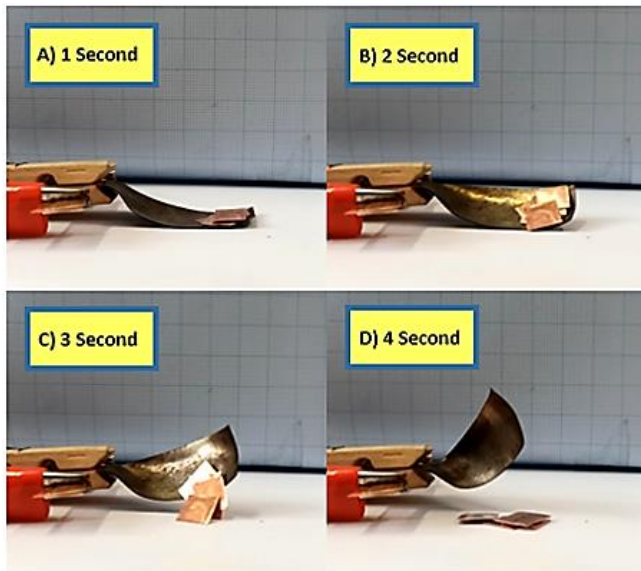


Figure 9. Lifting capacity measurement under 4 V DC

To assess the functional stability of the prepared IPMC, the actuator's displacement was monitored over time under a constant voltage of 4 V, as depicted in Figure 10. As observed, the displacement values exhibit a sharp decline within the first 4 minutes. During this initial phase, the actuator experiences significant deformation, leading to a rapid reduction in the surface resistance of the electrodes and an accelerated rate of solvent loss. Beyond this period, however, the rate of displacement decline slows considerably, and after approximately 20 minutes, the displacement values approach zero, causing the strip to cease movement. Based on these findings, it can be concluded that the functional stability of the prepared actuators, following immersion in water until reaching swelling equilibrium under a 4 V potential, lasts approximately 20 minutes [30-34].

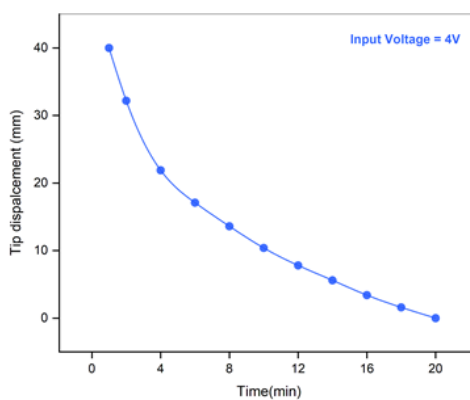


Figure 10. Tip displacement of the IPMC as a function of time under 4 V DC

#### 4. CONCLUSION

This research comprehensively covers the fabrication, characterization, and performance evaluation of IPMC actuators based on Nafion ion-exchange membranes. These actuators were prepared through four main steps: membrane pretreatment, ion exchange, primary reduction, and secondary reduction. The results of the analyses conducted on these actuators are as follows:



Scanning electron microscopy (SEM) analysis confirmed the successful formation of metal electrode layers on the membrane surface. The investigation of the water absorption parameter over time revealed that the minimum time required to reach the maximum level of absorbed water (equilibrium state) is approximately 16 hours. The surface resistance of the electrodes increased over time. This results in a decline in the performance of the IPMC actuator. Additionally, surface resistance values increased with distance from the tip of the strip.

The functional parameters of these actuators, such as displacement, maximum load capacity, durability, and blocking force, were dependent on the input voltages. As the input voltage increased, the displacement and force generated by the actuator also increased. However, due to the accelerated rate of solvent loss through evaporation and electrolysis, the operational durability of the actuator decreased. The maximum displacement of the IPMC actuator with dimensions of  $2 \times 6 \text{ cm}^2$  was measured 40 mm under a voltage of 4 V.

## REFERENCES

- [1] He, Qingsong, et al. "Review on improvement, modeling, and application of ionic polymer metal composite artificial muscle." *Journal of Bionic Engineering* 19.2 (2022): 279-298.
- [2] ul Haq, Mazhar, and Zhao Gang. "Ionic polymer–metal composite applications." *Emerging Materials Research* 5.1 (2016): 153-164.
- [3] Bhandari, Binayak, Gil-Yong Lee, and Sung-Hoon Ahn. "A review on IPMC material as actuators and sensors: fabrications, characteristics and applications." *International journal of precision engineering and manufacturing* 13 (2012): 141-163.
- [4] Jo, Choonghee, et al. "Recent advances in ionic polymer–metal composite actuators and their modeling and applications." *Progress in Polymer Science* 38.7 (2013): 1037-1066.
- [5] Shahinpoor, Mohsen, and Kwang J. Kim. "Ionic polymer–metal composites: I. Fundamentals." *Smart materials and structures* 10.4 (2001): 819.
- [6] He, Chendong, et al. "Preparation and modification technology analysis of ionic polymer–metal composites (IPMCs)." *International Journal of Molecular Sciences* 23.7 (2022): 3522.
- [7] Park, Si Won, et al. "Recent Progress in Development and Applications of Ionic Polymer–Metal Composite." *Micromachines* 13.8 (2022): 1290.
- [8] Tang, Gangqiang, et al. "A comprehensive survey of ionic polymer metal composite transducers: preparation, performance optimization and applications." *Soft Science* (2023).
- [9] Farid, Muhammad, et al. "Biomimetic applications of ionic polymer metal composites (IPMC) actuators-a critical review." *Journal of Biomimetics, Biomaterials and Biomedical Engineering* 20 (2014): 1-10.
- [10] Khmelnitskiy, Ivan K., et al. "Improvement of manufacture technology and investigation of IPMC actuator electrodes." *2017 IEEE Conference of Russian Young Researchers in Electrical and Electronic Engineering (EICONRUS)*. IEEE, 2017.
- [11] Wang, Yanjie, et al. "Effects of preparation steps on the physical parameters and electromechanical properties of IPMC actuators." *Smart Materials and Structures* 23.12 (2014): 125015.
- [12] Tiwari, R., and Kwang J. Kim. "IPMC as a mechanolectric energy harvester: tailored properties." *Smart Materials and Structures* 22.1 (2012): 015017.
- [13] Yu, Min, Hui Shen, and Zhen-dong Dai. "Manufacture and performance of ionic polymer–metal composites." *Journal of Bionic Engineering* 4.3 (2007): 143-149.
- [14] Wang, Yanjie, et al. "Effect of dehydration on the mechanical and physicochemical properties of gold-and palladium-ionomeric polymer–metal composite (IPMC) actuators." *Electrochimica Acta* 129 (2014): 450-458.
- [15] Khan, Ajahar, R. K. Jain, and Mu Naushad. "Development of sulfonated poly (vinyl alcohol)/polypyrrole based ionic polymer metal composite (IPMC) actuator and its characterization." *Smart Materials and Structures* 24.9 (2015): 095003.
- [16] Jin, Ning, et al. "Performance of ionic polymer–metal composite (IPMC) with different surface roughening methods." *Frontiers of Mechanical Engineering in China* 4 (2009): 430-435.
- [17] Wang, Yanjie, et al. "Effects of surface roughening of Nafion 117 on the mechanical and physicochemical properties of ionic polymer–metal composite (IPMC) actuators." *Smart Materials and Structures* 25.8 (2016): 085012.



- [18] Punning, Andres, Maarja Kruusmaa, and Alvo Aabloo. "Surface resistance experiments with IPMC sensors and actuators." *Sensors and Actuators A: Physical* 133.1 (2007): 200-209.
- [19] Ma, Suqian, et al. "High-performance ionic-polymer–metal composite: toward large-deformation fast-response artificial muscles." *Advanced Functional Materials* 30.7 (2020): 1908508.
- [20] Liu, H. G., K. Bian, and K. Xiong. "Large nonlinear deflection behavior of IPMC actuators analyzed with an electromechanical model." *Acta Mechanica Sinica* 35 (2019): 992-1000.
- [21] Liu, Hongguang, et al. "Experimental study and electromechanical model analysis of the nonlinear deformation behavior of IPMC actuators." *Acta Mechanica Sinica* 33 (2017): 382-393.
- [22] Li, Shufeng, and Joanne Yip. "Characterization and actuation of ionic polymer metal composites with various thicknesses and lengths." *Polymers* 11.1 (2019): 91.
- [23] Nasrollah, Amin, Hamid Soleimani, and Shadan Bafandeh Haghghi. "IPMC-based actuators: An approach for measuring a linear form of its static equation." *Heliyon* 10.4 (2024).
- [24] Yang, Liang, et al. "Models of displacement and blocking force of ionic-polymer metal composites based on actuation mechanism." *Applied Physics A* 126 (2020): 1-7.
- [25] Zhu, Zicai, et al. "Integrated fabrication process with multiple optimized factors for high power density of IPMC actuator." *International Journal of Smart and Nano Materials* 13.4 (2022): 643-667.
- [26] Yip, Joanne, et al. "Experimentally validated improvement of IPMC performance through alternation of pretreatment and electroless plating processes." *Smart materials and structures* 20.1 (2010): 015009.
- [27] He, Qingsong, et al. "Experimental study and model analysis of the performance of IPMC membranes with various thickness." *Journal of Bionic Engineering* 8.1 (2011): 77-85.
- [28] Yin, Guoxiao, et al. "Fabrication and performance analysis of high-performance cylindrical ionic polymer-metal composite actuators with various diameters." *Smart Materials and Structures* 31.11 (2022): 115003.
- [29] Liang, Yunhong, et al. "High Specific Surface Area Pd/Pt Electrode-Based Ionic Polymer–Metal Composite for High-Performance Biomimetic Actuation." *ACS Sustainable Chemistry & Engineering* 10.8 (2022): 2645-2652.
- [30] Yu, Chung-Yi, Yi-Wei Zhang, and Guo-Dung J. Su. "Reliability tests of ionic polymer metallic composites in dry air for actuator applications." *Sensors and Actuators A: Physical* 232 (2015): 183-189.
- [31] Yamakita, Masaki, et al. "A snake-like swimming robot using IPMC actuator and verification of doping effect." *2005 IEEE/RSJ international conference on intelligent robots and systems. IEEE*, 2005.
- [32] Bar-Cohen, Yoseph, et al. "Challenges to the application of IPMC as actuators of planetary mechanisms." *Smart structures and materials 2000: electroactive polymer actuators and devices (EAPAD)*. Vol. 3987. SPIE, 2000.
- [33] Chen, Zheng, Tae I. Um, and Hilary Bart-Smith. "A novel fabrication of ionic polymer–metal composite membrane actuator capable of 3-dimensional kinematic motions." *Sensors and Actuators A: Physical* 168.1 (2011): 131-139.
- [34] Hasani, Mehdi, et al. "Fabrication of ionic polymer-metal composite actuators with durable and quality-enhanced sputtered electrodes." *Journal of Micromechanics and Microengineering* 29.8 (2019): 085008.

**Graphical abstract**